Spatial Tree Mapping Using Photography

Adam R. Dick, John A. Kershaw, Jr., and David A. MacLean

ABSTRACT

Stem maps describing the spatial location of trees sampled in a forest inventory are used increasingly to model relationships between neighboring trees in distance-dependent growth and yield models, as well as in stand visualization software. Current techniques and equipment available to acquire tree spatial locations prohibit widespread application because they are time-consuming, costly, and prone to measurement error. In this report, we present a technique to derive stem maps from a series of digital photographs processed to form a seamless 360° panorama plot image. Processes are described to derive distance from plot center and azimuth to each plot tree. The technique was tested on 46 field plots (1,398 sample trees) under a range of forest conditions and compared with traditional methods. Average absolute distance error was 0.38 ± 0.44 m, and average absolute azimuth error was 2.3 ± 2.5°. Computed average horizontal accuracy was 0.40 ± 0.42 m, with 85% of measured trees being within 0.5 m of the field-measured tree location.

Keywords: stem mapping, mensuration, forest inventory, 360° plot photographs

Landowners and land managers routinely conduct forest inventories and use plots to monitor changes over time. Traditional forest inventories focused primarily on characterizing timber conditions, but over time, forests have increasingly been recognized as providers of a wide suite of economic, environmental, and social products and services (Agee and Johnson 1988, Gillis 1990, Christensen et al. 1996). In response, inventory design and parameters measured have changed to address questions about forest conditions. Typically, forest inventories have two primary purposes: to provide a snapshot of forest conditions and to provide information on the rate of growth or change of these conditions over time. Such data are often used to calibrate growth and yield models, which are subsequently used to predict change in forest conditions over time, often in response to management activities.

As our understanding of complex interactions influencing tree growth has increased, so has the complexity of growth and yield models and their calibration. One parameter increasingly included in models is tree spatial location (Tome and Burkhart 1989, Biging and Dobbertin 1992, Kokkila et al. 2006). Information on tree spatial location is not widely collected or is collected only for specialized inventory designs. Current methods to map tree locations limit widespread use because they are expensive and time-consuming. Equipment can range from a compass and measuring tape to laser systems with integrated electronic compasses or global positioning systems (GPSs). Although GPS accuracy has improved and costs have declined in recent years, GPS is still prone to loss of accuracy or functionality under forest canopies, especially if the unit is held close to the tree bole to make measurements. The use of a compass and measuring tape, although cost-effective, is prone to measurement error and is time-consuming. Laser systems are accurate but expensive and need frequent calibration to ambient conditions to ensure accuracy.

Photography has long been recognized as an important forestry tool. Aerial photography and photointerpretation, in many cases, serve as the foundation on which forest inventories are designed (Congalton and Green 1999). Although foresters are familiar with photography and other remotely sensed data sources above canopy, ground-based photographic techniques are infrequently used.

Reineke (1940) explored using repeated photographs of permanent sample plots to show changes in plot conditions over time. The "stereodendrometer" (Bartorelli and Cantiani 1962) used a stereo pair of cameras to determine tree diameters and heights. Grosenbaugh (1963) provided an overview of optical dendrometers and presented the theory for their use, including photographic applications. Clark et al. (2000) updated the recent advances in the development of optical dendrometers. Hall (2002a, 2002b) used photographic methods to measure change in vegetation conditions over time and to measure shrub density. The methods were applied mostly in rangeland conditions or open forest conditions.

Recent advances in digital camera technology have resulted in inexpensive consumer-grade cameras that produce high-quality images at low cost. Digital storage media and computing power have also advanced, so that large numbers of images can be efficiently stored and processed. In this report, we describe a method to acquire photographs of forest sample plots and apply processing techniques to determine spatial locations of the sample trees observed in the photographs. We also assess accuracy of the photo-based method against a traditional method for making these measurements. Whereas past work on the use of optical dendrometers focused on their use to measure individual tree dimensions, the work we present focuses on measuring spatial location.

Manuscript received July 10, 2009, accepted January 13, 2010.

Adam R. Dick (adam.dick@gnb.ca), New Brunswick Department of Natural Resources, New Brunswick Growth and Yield Unit, P.O. Box 6000, 1350 Regent Street, Fredericton, New Brunswick E3B 2G6, Canada. John A. Kershaw, Jr., and David A. MacLean, Faculty of Forestry and Environmental Management, P.O. Box 4400, University of New Brunswick, Fredericton, New Brunswick E3B 6A3, Canada. *The authors thank Gaetan Pelletier of J.D. Irving, Ltd., for providing equipment, accommodation, and access to the Black Brook District during fieldwork, as well as Luke Amos-Binks, Chris Griffin, and Arthur James Perry for assistance with fieldwork. The Canada Sustainable Forest Management Network Centre of Excellence and J.D. Irving, Ltd., funded this research. We also acknowledge the suggestions from three anonymous reviewers.*

This article uses metric units; the applicable conversion factors are: centimeters (cm): 1 cm = 0.39 in.; meters (m): 1 m = 3.3 ft; square meters (m^2): 1 m^2 = 10.8 ft^2; hectares (ha): 1 ha = 2.47 ac.

Table 1. Summary of characteristics of 46 plots sampled for photo assessment in northern New Brunswick.

Stand type	No. of plots	QMD[a]		Density		Basal area		Stand composition	
		$\bar{x}$	SD	$\bar{x}$	SD	$\bar{x}$	SD	SW	HW
		.....(cm).....		.....(stems ha^{-1}).....		.....(m^2).....		.....(%).....	
Hardwood	17	21.1	4.2	737.6	306.4	23.3	5.5	3.2	96.8
Mixedwood	14	21.2	2.7	809.1	317.6	26.9	8.6	61.4	38.6
Softwood	10	18.8	2.2	1,363.0	503.1	36.2	10.5	97.4	2.6
Softwood plantation	5	19.7	1	1,075.5	203.7	32.6	4.3	100	0

[a] QMD, quadratic mean diameter; SD, standard deviation; SW, softwood; HW, hardwood.

Materials and Methods

Study Location

Sample plots were located on the J.D. Irving, Ltd., Black Brook District in northwestern New Brunswick, Canada (47°00′ to 47°30′N, 67°20′ to 68°10′W). The District is 190,000 ha and represents some of the most intensively managed forests in Canada. Sample plots were a subset of plots established as part of a harvesting trial. Plots were established on a systematic grid across the study area, and a subset was selected for this study to represent a range of stand conditions, densities, species compositions, and management regimes. Sampled plot characteristics are summarized in Table 1.

Plot Establishment

Tree Mapping

Sample plots were established as variable-radius plots using a 1-m^2 ha^{-1} basel area factor (BAF) angle gauge (1 m^2 ha^{-1} = 4.356 ft^2 ac^{-1}). The distance from plot center to each tallied tree (nearest 0.1 m) and the azimuth (nearest degree) were measured using a tape measure and compass mounted on a tripod and recorded in a field data collector. Distances were measured from plot center to the face of the tree. The dbh (to the nearest 0.01 m) of tallied trees was measured using tree calipers. Using recorded distance and tree diameter, the field data collector computed whether measured trees were in or out of the tally. This capability was useful in the field for assessing trees that were borderline based on the angle gauge. The tally sweep began at north azimuth (0°) and continued clockwise around the plot.

Photo Measurements

We evaluated tree distance measurements on photos using two methods: a) targets placed on trees; and b) tree dbh measured from the photograph. After measuring all trees, a target printed on card stock 21.6 × 27.9 cm was placed on each tree at breast height (1.3 m). In the center of each target was a 17.8 × 17.8-cm black square, and printed above this was an indexing tree number to relate photographic measurements to field measurements. The targets are not required to make the measurements and can be considered optional; however, it is important to have a method for indexing trees in the photos to tallied attributes.

A digital camera mounted in portrait orientation on a panoramic tripod mount (Kaidan Kiwi) was placed on a tripod 1.3 m directly above the plot center. The panoramic tripod mount ensured that the camera's focal point was directly above the rotational axis of the tripod, such that the resulting series of photographs could be stitched together with minimum distortion. The degree index on the mount was used to determine accurate camera rotation between photographs. Two camera models were used, an Olympus D550z (3 megapixels) and a Canon PowerShot SD200 (3.2 megapixels). Both cameras are entry-level "point-and-shoot" type cameras with a replacement cost between $150 and $200 each.

The first plot photograph was taken oriented toward the first tree measured, and a series of 24 photographs, taken at 15° intervals around plot center, was then obtained. The 15° interval provided sufficient overlap between adjacent photographs to minimize distortion in the stitched panoramic image. Camera setup and photography averaged approximately 5 minutes per plot.

Postprocessing

Photographs were downloaded from the camera to a computer and organized into folders by plot. A software program called The Panorama Factory (Smoky City Design, LLC) was used to stitch

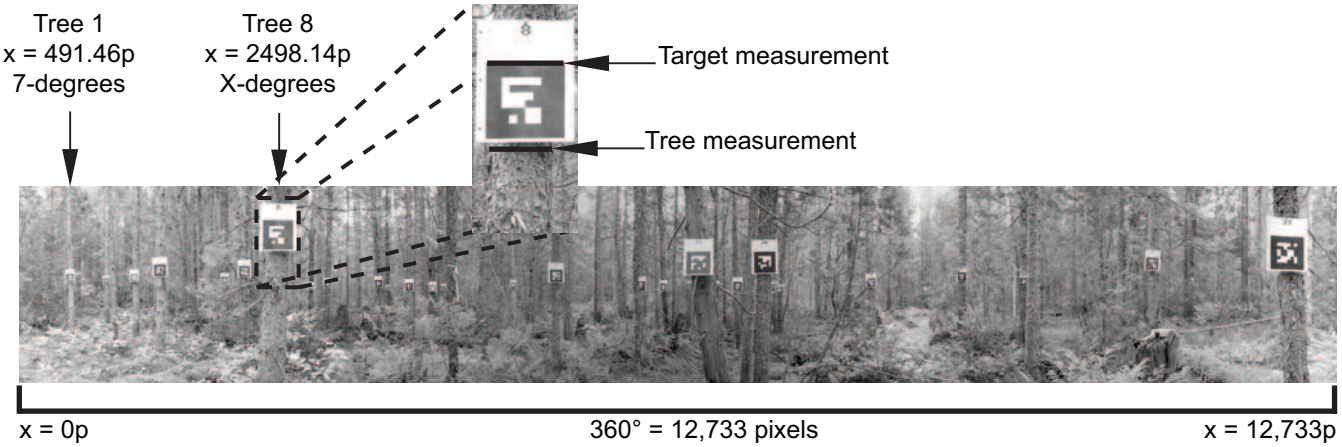

Figure 1. Example of panoramic image produced and an overview of the measurements and dimensions used in distance and azimuth calculations.

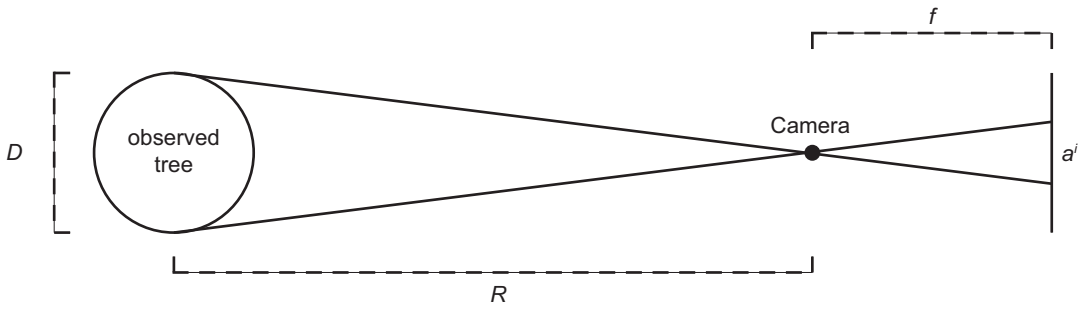

Figure 2. Relationship between field and photo measurements, including tree diameter (*D*), distance between tree and plot center (*R*), camera focal length (*f*), and width of observed tree on the image (a^i). Camera location is at plot center.

each set of plot photographs together. The stitching process averaged less than 10 minutes per plot on a Pentium 4 (2.3 GHz) computer with 1 GB of RAM. The resulting panoramic images show a 360° view of each plot. With proper field setup, sufficient overlap between adjacent images, and geometric adjustments made by the software, the panoramic images have minimal distortion.

Panoramic images were saved as JPEG files, and subsequent measurements were performed using ArcMap 9.2 GIS software (ESRI, Redlands, CA). The panoramic images were imported into ArcMap, and a line feature shapefile was created containing attribute fields to store tree information, including plot number, tree number read from targets on the trees, and measurement type. Figure 1 shows a sample panoramic image and describes measurements made from the photographs. In Figure 1, the black target square is filled with a checkerboard pattern that was not evaluated or used in this report; only the outer perimeter of the black square was used. For every tree, there was the possibility of making two measurements: tree width (diameter) at breast height and target width; these are depicted by black lines in Figure 1. Measurements of either tree width or target width were made only if there was an unobstructed view of the edges of the feature and accurate measurements could be made. If both measurements were possible, then both were made. Trees completely obscured by other trees or understory vegetation could not be measured, and no information was recorded for these. Measurements were made by drawing a line from edge to edge of the tree diameter or target, and, using the geometry calculator feature in ArcMap, minimum and maximum *x*-coordinate (Xmin and Xmax), line length (a^i) and line midpoint (Xmid) were calculated for each line feature created. All values were recorded in number of pixels. When all measurements were complete, the shapefile attribute table was exported to an Access database, and photo measurements were related to field-measured dbh by plot number and tree number.

Calculations from Measurements

It was possible to calculate distance between plot center and each tree two ways, using either tree width or target width as input. In both cases, distance from plot center to each tree (R) was calculated by multiplying the ratio between actual size of a feature (D) and size of the feature in the photograph (a^i) by focal length (f) of the camera (Figure 2),

$$R = \left(\frac{D}{a^i}\right) \times f. \qquad (1)$$

To calculate distance using measurement of tree width in the photo, it is necessary to have measured tree dbh in the field. In this case, dbh was substituted for D in Equation 1, and a^i was tree width measured on the photograph. Although the targets are not essential to

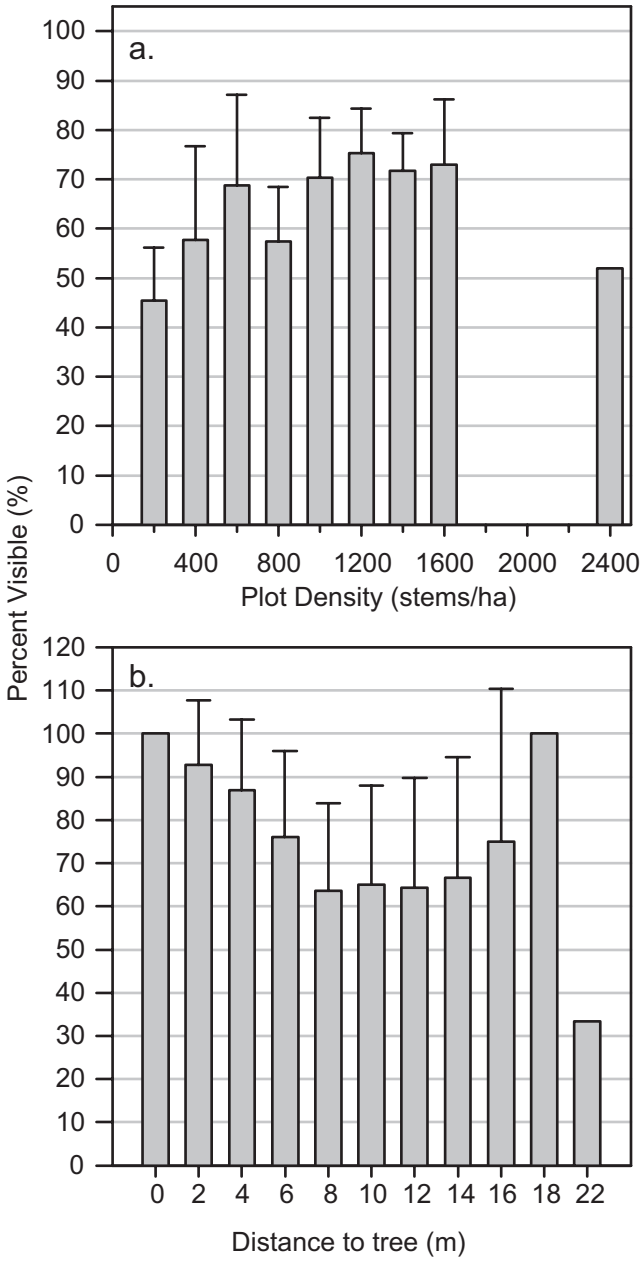

Figure 3. Percentage of trees visible in plots by plot density (a) and distance to plot center (b).

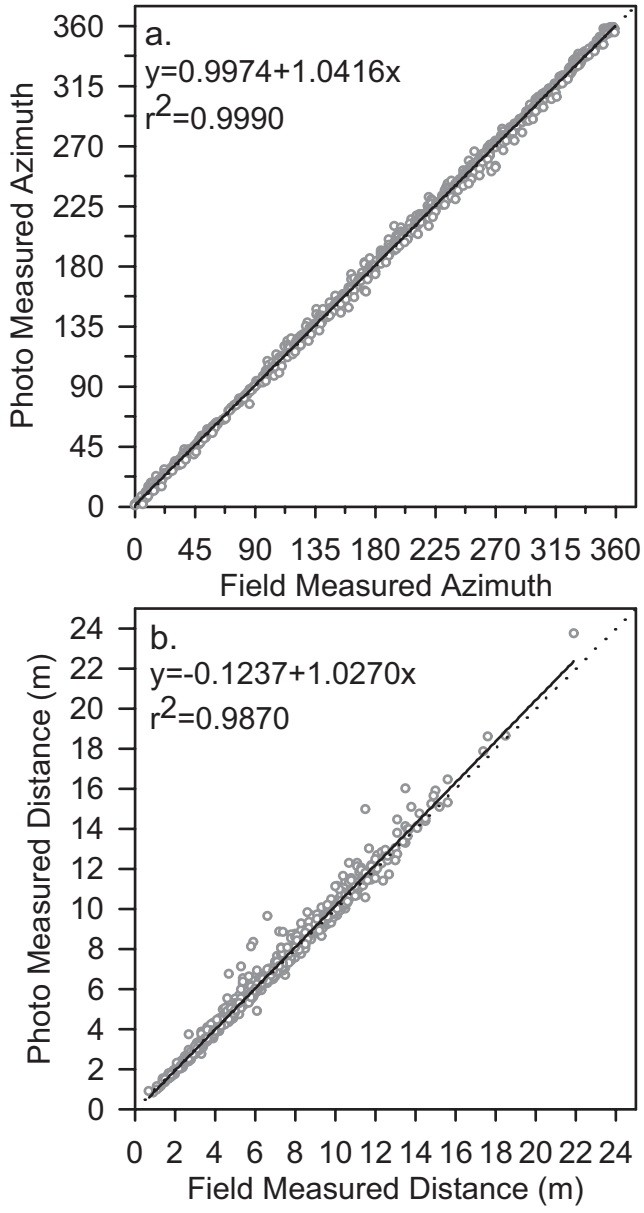

Figure 4. Regressions of field and photo-based azimuth measurements (a) and distance measurements (b).

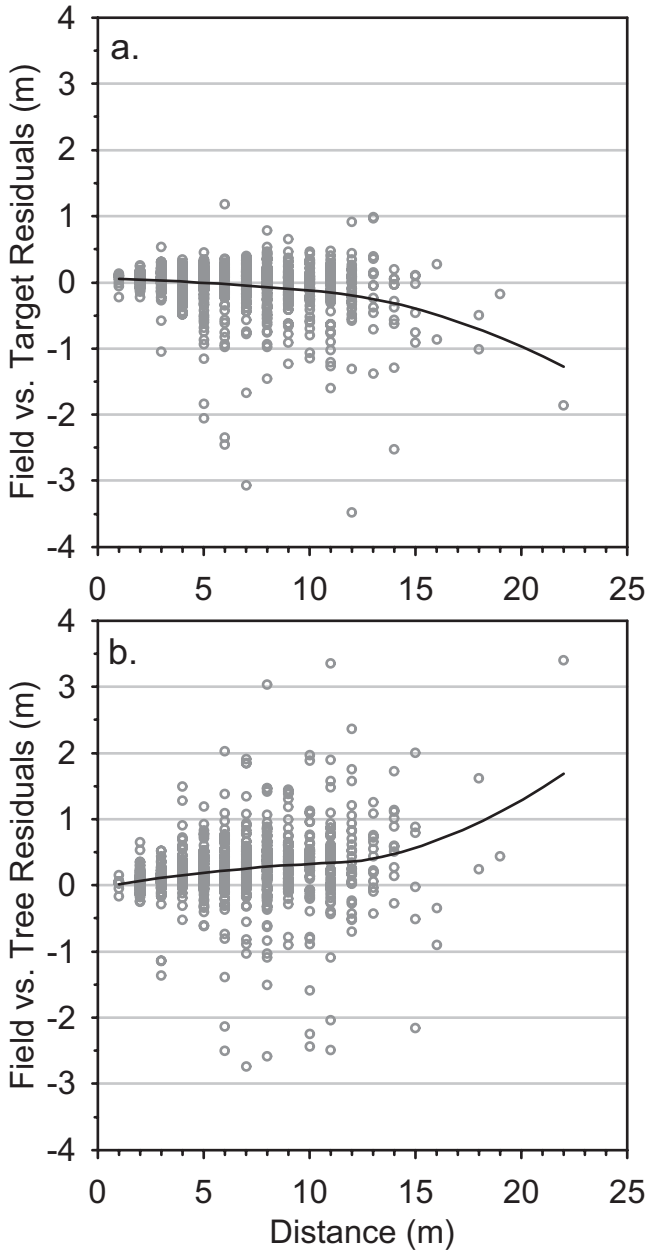

Figure 5. Residual errors resulting from regressions between field- and photo-based distance measurements when photo measurements were derived from targets placed on trees (a) and tree dbh measured from the photograph (b).

distance calculations using tree width measurements, the numbers appearing on the targets are helpful to relate field measurements to photo measurements of individual trees. To calculate distance using measured target width, D was actual target width (17.8 cm), and d^i was target width measured on the photograph. This is especially convenient because it means that no measurements of the tree are required in the field to determine distance between trees and plot center. If the distance from tree to plot center (R) is calculated using the target measurement, and tree width is measured in the photo (d^i), then the actual tree dbh (D) can also be computed, by rearranging Equation 1.

Azimuth (θ) from plot center to each tree was calculated using measurements from the panoramic images, with only azimuth of the first tree measured in the field to initialize measurements. The panoramic images have a constant radial (azimuth) scale (degrees per pixel), determined by dividing 360° by the width of the image in pixels. The first tree in the image was assigned the azimuth measured in the field. Azimuths of other trees were determined based on pixel distances of line midpoints (Xmid) between the first tree and all other trees multiplied by radial scale (degrees per pixel) to estimate angle from first tree. Using Figure 1 as an example, radial scale was 0.028°/pixel. Pixel distance between tree 8 and tree 1 was 2006.68 pixels (2498.14 p − 491.46 p); therefore, tree 8 is 56.2° from tree 1 (2006.68 × 0.028) and 63.2° azimuth (56.2° + 7°).

With distance and azimuth values calculated, X and Y coordinates for each tree were calculated using

$$X = R \cos \theta \quad (2)$$

and

$$Y = R \sin \theta. \quad (3)$$

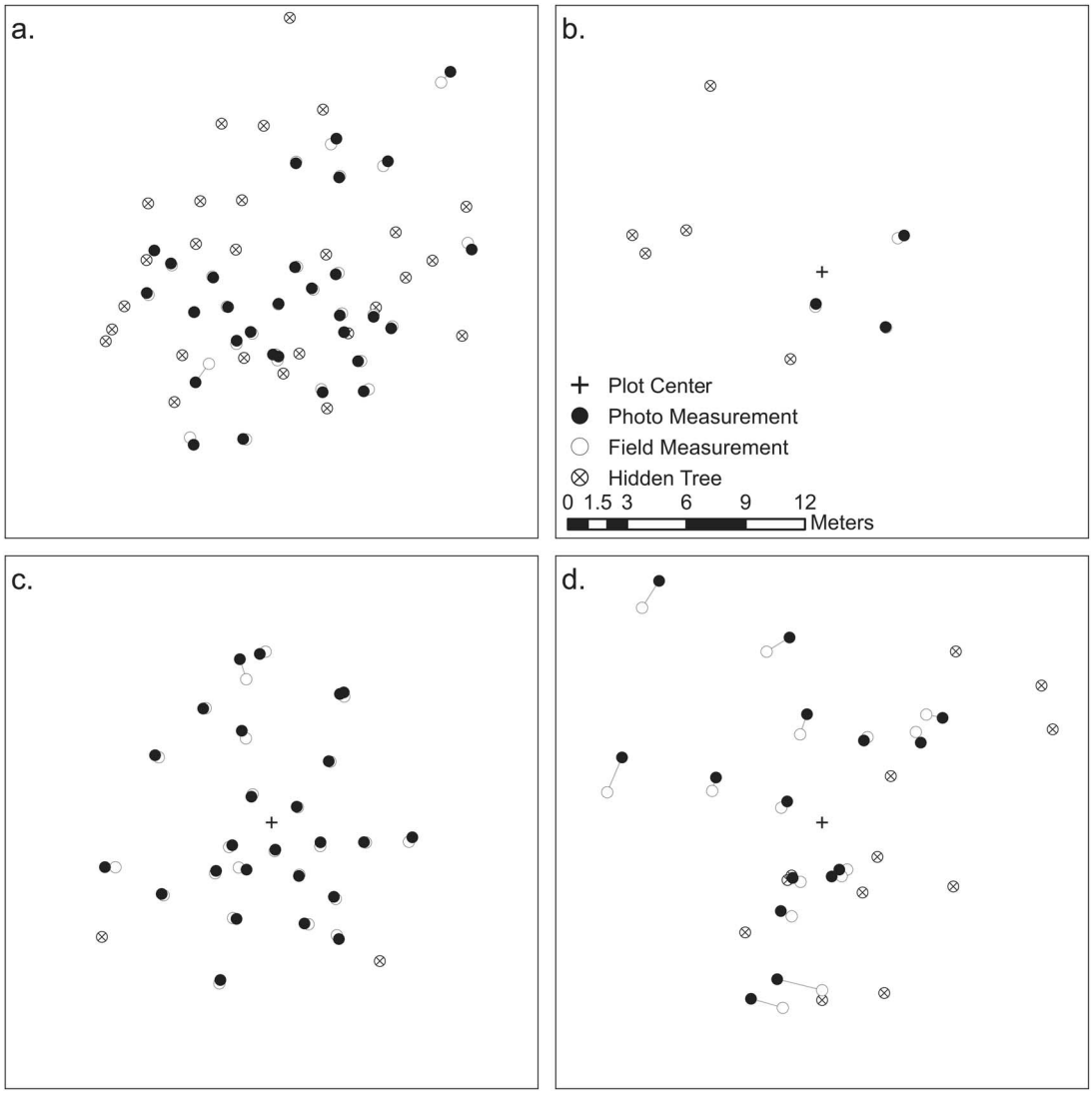

Figure 6. Maps showing examples of plotted stem maps. Crosses represent plot center, solid circles represent tree locations derived from photographs, and open circles represent field measurements. Lines connect the two measurement sources for the same tree. Circles filled with crosses mark field locations of trees not visible in the photographs. Plots shown include those with the highest density (a), lowest density (b), most visible trees (c), and highest distance and azimuth errors (d).

Table 2. Descriptive statistics of sample plots shown in Figures 6 and 7.

	Plot			
	a	b	c	d
Number of trees/plot	56	8	27	27
% Visible	52	38	93	59
Density (no./ha)	2462	149	975	950
QMD (cm)[a]	17.02	26.19	18.78	19.02
Mean error distance (m)	0.20	0.18	0.27	0.99
Mean error azimuth (°)	0.9	0.00	1.48	7.87
% Softwood	92	63	100	20
% Hardwood	8	37	0	80

[a] QMD, quadratic mean diameter.

X and Y coordinates were also calculated from the field measurements. It is important to note that azimuth measurements in the field were made in a clockwise direction from north (north = 0). Under the polar coordinate system, azimuths are measured in a counterclockwise direction from east (east = 0). Field measurements were converted from azimuth to polar angle before being entered into the above formulas using the procedures in Wilson (2000).

Distances between field and photo derived coordinates were calculated as

$$\text{Distance} = \sqrt{((x_{\text{photo}} - x_{\text{field}})^2 + (y_{\text{photo}} - y_{\text{field}})^2)}. \quad (4)$$

The calculated distance represents the combined errors of radial distance and azimuth measurements, and it represents the horizontal accuracy of photo-derived tree locations relative to the field-derived ones. Average distance, which can be considered analogous to root mean squared error (RMSE), for each plot was calculated as

$$\text{RMSE}_{\text{plot}} = \sqrt{\sum_{i=1}^{n} \frac{((x_{\text{photo},i} - x_{\text{field},i})^2 + (y_{\text{photo},i} - y_{\text{yield},i}))^2}{n}}. \quad (5)$$

Calculated RMSE for each plot provides a measure of the aggregated plot measurement accuracy.

Figure 7. Photographs of the plots mapped in Figure 6, from which the photo measurements were derived.

Results

A total of 46 plots were sampled across a range of stand types, including five in 25-year-old black spruce (*Picea mariana* [Mill.] BSP) plantations. Density ranged from 740 to 1,360 stems/ha, basal area ranged from 23 to 36 $m^2\ ha^{-1}$, and softwood composition ranged from 3 to 100% (Table 1).

Tree Visibility

One important issue is trees hidden from view in the panoramic image, when behind or overlapped by adjacent trees, if there is dense understory vegetation, or if trees are located a long distance from the camera. These issues are not unique to the photographic technique, but using photographs it is impossible to physically move understory vegetation or walk behind trees, as is possible in the field. There was no clear relationship between proportion of visible trees and stand density (Figure 3a). This may result from an interaction between stand density and understory vegetation: as stand density decreases, understory vegetation increases, and this may be a larger contributing factor to hidden trees than obstruction by other trees, since tree visibility increased as stand density increased (Figure 3a).

There was a clear trend of a decreasing percentage of trees visible as distance from plot center increased from 0 to 8 m (Figure 3b). The percentage of trees visible was constant from 8 to 14 m from plot center and then increased at 16–18-m distances. This increase was based on a few observations, almost exclusively large-diameter tolerant hardwood trees in low-density conditions. Since the plots were of variable radii, small trees were excluded from the tally at increasing distances.

Photo Measurements

In total, 881 trees were visible in the 46 plot panoramas, and these were used to calculate distance and azimuth from plot center and compared with field-collected measurements. Photo-estimated azimuths and distances compared well with field-collected values (using tree widths from photos), with r^2 values of 0.99 for azimuths and 0.98 for distances ($P < 0.0001$ in both cases) (Figure 4). Average absolute error for azimuth measurements was $2.3 \pm 2.5°$, with 46 and 68% of measured trees within ± 1 degrees and ± 2 degrees of error, respectively. For both variables, relationships between estimated and measured values were consistent across the range of measurements with minimal bias.

Residuals for the distance measurement regressions were compared using distances estimated from both target measurements (Figure 5a) and tree measurements (Figure 5b) on the photos. The locally weighted regression line (LOESS, Cleveland 1981) shows that for estimates made with target measurements, there was a tendency to underestimate distance as trees were farther from plot center. The opposite was the case when tree measurements were used. In both cases, however, inflection points where errors increased occurred about 15 m from plot center, which is typically beyond the size of most fixed-area inventory plots. The distribution of errors was less variable using measurements based on targets versus trees. Tree measurements include errors associated with field measurements, image measurements, and tree eccentricity. With target measurements, actual target width is a known constant, is easier to identify on the images, and consequently leads to lower measurement error. The average absolute error for distance measurements was 0.23 ± 0.32 m using target measurements (66 and

80% within ±0.1 and ±0.2 m, respectively) and 0.38 ± 0.44 m using tree measurements (42 and 57% within ±0.1 and ±0.2 m).

Figure 6 presents four examples of generated tree maps for plots selected to display a variety of conditions sampled, as well as mapping accuracy, including plots with the highest and lowest densities, highest visibility, and highest error. Table 2 summarizes stand characteristics and mapping accuracy for each plot, and Figure 7 shows the 360° panoramic photos for these plots. Trees visible ranged from 38% (Figure 6b) to 93% (Figure 6c), and density ranged from 149 stems/ha (Figure 6b) to 2,460 stems/ha (Figure 6a). Mean distance error ranged from 0.18 to 0.27 m for three plots but was 0.99 m for the fourth (Figure 6d), which also had the largest azimuth error, at 7.9° versus 0–1.4° for the other three plots shown (Table 2). There was a large amount of topographic relief in the plot in Figures 6d and 7d, which contributed to the high error. Again, this is not unique to this technique; slope corrections are routinely applied in normal field techniques. The topography of the plot will need to be taken into consideration when determining whether photography techniques are applicable.

The average tree horizontal accuracy was 0.40 ± 0.42 m. Fifty-six percent of trees were within 0.3 m of the field-measured location, 68% were within 0.4 m, and 85% were within 0.5 m. Average plot RMSE calculation was 0.53 ± 0.23 m; 37% of plots were within 0.4 m, 52% were within 0.5 m, 72% were within 0.6 m, and 78% were within 0.7 m.

Discussion and Conclusions

In this report, we present a new technique for spatially mapping trees in photographed plots. The camera equipment and postprocessing software used are inexpensive compared with other tools used for tree mapping. Recent innovations in digital cameras and improvements in computer storage and processing power make this technique viable operationally. We believe that the methods presented have the potential to serve alongside remotely sensed data sources commonly used by forest managers, such as aerial photography, satellite imagery, and light detection and ranging.

Although a time study was not conducted to determine relative efficiency of the photo-based technique compared with existing methods, on the basis of our experience, we believe that it is less time-consuming. The tags placed on trees increased accuracy, but this should be weighed against the additional time required to place and remove tags on trees. Readily available and inexpensive higher-resolution cameras may decrease differences between using and not using tags. For this study, postprocessing of photo data was mostly done manually; however, existing digital image processing tools can likely be adapted to automate most steps.

One issue that needs to be addressed with this technique is hidden trees. Although this problem is not unique to photo-based measurements, there are simply limitations to what can be done after the fact to improve visibility of hidden trees. It is not possible to move understory vegetation in the photo or walk behind trees to see what might be concealed behind. To minimize the effect of hidden trees, plot design should take into consideration effects of stand density, understory vegetation density, and plot size on visibility of trees in photographs. Ultimately, if the camera techniques can be adapted such that measurements are automated and are completed "live" in the field, then field technicians could temporarily move understory vegetation that obscures the camera view. Multiple overlapping plots and mapped plots would provide multiple observations of sample trees; the plot can be generated from the combined observations, or a larger plot size can be sampled. It is also worth mentioning the utility of the generated photographs as a standalone tool to aid stand visualization and to monitor stand change over time.

Given the accuracy of stem-mapped trees, with average plot center to tree distance errors of 0.38 ± 0.44 m, average azimuth errors of 2.3 ± 2.5°, and horizontal accuracies of 0.40 ± 0.42 m, this photo-based method is worth considering in cases where individual tree locations in permanent sample plots are desired.

Literature Cited

AGEE, J.K., AND D.R. JOHNSON. 1988. *Ecosystem management for parks and wilderness.* University of Washington Press, Seattle, WA.

BARTORELLI, U., AND M. CANTIANI. 1962. The stereodendrometer. *Ital. For. Mont.* 17(5):170–182.

BIGING, G.S., AND M. DOBBERTIN. 1992. A comparison of distance-dependent competition measures for height and basal area growth of individual conifer trees. *For. Sci.* 38:695–720.

CHRISTENSEN, N.L., A.M. BARTUSKA, J.H. BROWN, S. CARPENTER, C. DANTONIO, R. FRANCIS, J.F. FRANKLIN, J.A. MACMAHON, R.F. NOSS, D.J. PARSONS, C.H. PETERSON, M.G. TURNER, AND R.G. WOODMANSEE. 1996. The report of the Ecological Society of America Committee on the Scientific Basis for Ecosystem Management. *Ecol. Applic.* 6:665–691.

CLARK, N.A., R.H. WYNNE, AND D.L. SCHMOLDT. 2000. A review of past research on dendrometers. *For. Sci.* 46(4):570–576.

CLEVELAND, W. 1981. LOWESS: A program for smoothing scatterplots by robust locally weighted regression. *Amer. Stat.* 35:54.

CONGALTON, R.G., AND K. GREEN. 1999. *Assessing the accuracy of remotely sensed data: Principles and practices.* CRC Press, Boca Raton, FL.

GILLIS, A.M. 1990. The new forestry: An ecosystem approach to land management. *Bioscience* 40:558–562.

GROSENBAUGH, L.R. 1963. *Optical dendrometers for out-of-reach diameters: A conspectus and some new theory. For. Sci.* Monograph 4. 47 p.

HALL, F.C. 2002a. *Photo point monitoring handbook: Part A—Field procedures.* US For. Serv. Gen. Tech. Rep. PNW-GTR-526A. 48 p.

HALL, F.C. 2002b. *Photo point monitoring handbook: Part B—Concepts and analysis.* US For. Serv. Gen. Tech. Rep. PNW-GTR-526B. 134 p.

KOKKILA, T., A. MAKELÄ, AND A. FRANC. 2006. Comparison of distance-dependent and distance-independent stand growth models is perfect aggregation possible? *For. Sci.* 52:623–635.

REINEKE, L.H. 1940. Permanent sample plot photography. *J. For.* 38:813–815.

TOME, M., AND H. BURKHART. 1989. Distance-dependent competition measures for predicting growth of individual trees. *For. Sci.* 35:816–831.

WILSON, A.D. 2000. *New methods, algorithms, and software for rapid mapping of tree positions in coordinate forest plots.* US For. Serv. Res. Pap. SRS-19. 27 p.